PERIODICA POLYTECHNICA SER. TRANSP. ENG. VOL. 22, NO. 3-4, PP. 207-223 (1994)

FLOW METER OPTIMIZATION BY USER DEFINED NONLINEAR FINITE ELEMENT

Ferenc TAKÁCS* and György TÓTH**

* Department Transport Engineering Mechanics
Technical University of Budapest
H–1521 Budapest, Hungary
** T&T Data Automation Ltd
H–1116 Budapest, Hunyadi M. u. 32. Hungary

Abstract

Authors have developed a nonlinear pipe element for MMG Co. Ltd who is owner of several patents pending of flow meters in order to take into account the Coriolis forces produced by the flow of fluids in vibrating pipes. The aim of the development is to improve the construction of existing Coriforce flow meters where the measuring method is based on the presence of Coriolis forces which are in linear relation with the mass flow in pipes. The paper discusses the modelling aspects and shows industrial example as well.

Keywords: nonlinear finite element, Coriolis force, flow meter.

1. Introduction

Direct flow meters based on Coriolis forces were developed dynamically during the last decade. These are direct means that we do not have to measure density and volume flow separately and compute the mass flow indirectly. As the mass flow induces Coriolis forces, measurement of these forces lets us know the mass flow in a direct way. The main advantage of Coriolis flow meters is that in a large measuring range (turn-down ratio 1/20) we can measure the mass flow with a 0.2% accuracy independently of the fluid consistency (physical state, viscosity, density). As we do not have moving parts we can achieve high reliability, stability and life expenditure. Therefore Coriolis flow meters are going to replace indirect flow meters on more and more fields of use.

Development of vibrating Coriolis flow meters has produced a big variety of pipe forms and vibrating methods. Most of solutions can be characterized by the following remarks:

Every cross section of a pipe constrained at its extremities and excited with its eigenfrequency is moving on an arched path, therefore for every cross section there is a periodic angular velocity.

Consequently, the Coriolis forces produced by mass flow in the pipe and the above mentioned angular velocity will be periodic of the same

frequency which will excite periodic vibration of the pipe. This vibration is due only to mass flow and it will be superposed on excited vibration.

One can always find two points along the length of the pipe where the phase shift of the vibrations shows only the effects of Coriolis forces, depending on mass flow. The phase shift of the two sinusoidal signals is the output of the flow meters.

The design of optimal flow meters is to determine the optimal values of numerous parameters which are function of the others. We mention only the most important parameters here:

- geometry of vibrating pipe
- material of pipe
- vibrating mode
- position and mass of sensors mounted on pipe
- measuring range
- error rate of signal processing (error of signal processing divided by the total errors of the flow measurement)
- damping and effect of vibration loss (mechanical coupling with the environment, balancing)
- effect of outer mechanical noise
- effect of static and dynamic mechanical loads (pressure dependency, fatigue)
- pressure loss

We have two solutions for the flow meter optimal design:

1. Analysis of measurements of one or more prototypes. This process is highly interactive and requires sequent modification and measurement of prototypes.
2. State a numerical model of the physical problem and find optimal values of the model parameters.

MMG Co. Ltd has made economic efficiency estimations for both methods. These estimations have made MMG Co. Ltd. purchase Systus finite element software as a tool for the second method. Two major arguments have influenced this decision:

First: Construction of large prototypes is time consuming and expensive.

Second: As even largest finite element softwares do not include Coriolis pipe elements authors have developed a new element to be linked with Systus shared library. Our paper shows the most important steps of element derivation and compares its behaviour with theoretical test and industrial measurements.

Nomenclature

A	cross section
$[\mathbf{B}]$	damping matrix
E	Young modulus
G	shear modulus
I	area moment of inertia
k	Timoshenko shear coefficient
$[\mathbf{K}]$	stiffness matrix
L	length of pipe
$[\mathbf{M}]$	mass matrix
$\mathbf{N}$	shape function vector
$\mathbf{q}$	nodal variable vector
S	Hamilton functional
t	time
T	kinetic energy
τ	integration time step
Δt	time shift of zero crossing
U	potential energy
v_0	mean velocity of fluid
x	distance along pipe axis
α	shear strain
Θ	rotation due to flexural deformation
ω	angular velocity
φ	circumferential angle

Subscripts

f fluid quantities

p pipe quantities

Superscripts

(e) elemental quantities

T transpose

2. Derivation of Coriolis Pipe Element

The Coriolis forces effect only the transverse vibration of the fluid--conveying pipe therefore we show only the derivation of finite element formulation of these equations of motion by Hamilton's principle. For Hamilton's principle we have the functional

$$S = \int_0^t (T - U)dt \, .$$

We introduce Θ as a rotation due to flexural deformations and α as shear strain. We assume that the slope of the pipe neutral axis $\partial u/\partial x$ can be written in the form

$$\frac{\partial u}{\partial x} = \Theta + \alpha \ .$$

This is a usual form for Timoshenko beams. With the above assumptions the potential energy of the pipe is the following

$$U_p = \frac{1}{2} \int_0^L \left[EI_p \left(\frac{\partial \Theta}{\partial x} \right)^2 + kGA_p \alpha^2 \right] dx \ .$$

Similarly the kinetic energy can be expressed in terms of transitional and rotational inertia

$$T_p = \frac{1}{2} \int_0^L \left[\rho_p A_p \left(\frac{\partial u}{\partial t} \right)^2 + \rho_p I_p \left(\frac{\partial \Theta}{\partial t} \right)^2 \right] dx \ .$$

The energy contribution of the fluid was formulated from Timoshenko perspective. We neglected the effect of internal pressure on potential energy and assume that the fluid contributes only kinetic energy. This contribution was formulated as follows

$$T_f = \frac{1}{2} \int_0^L \left[\rho_f A_f \left(\frac{\partial u_f}{\partial t} \right)^2 + \rho_f I_f \left(\frac{\partial \Theta}{\partial t} \right)^2 \right] dx \ .$$

Transverse fluid velocity $\partial u_f/\partial t$ is related to the transverse velocity of the pipe $\partial u/\partial t$, through the material derivative. The material derivative relates the Eulerian description of the fluid to the Lagrangian description of the pipe by the following:

$$\frac{\partial u_f}{\partial t} = v_0 \frac{\partial u}{\partial x} + \frac{\partial u}{\partial t} \ .$$

The axial fluid velocity v_0 was assumed to be independent of x and to be constant across the cross section of the pipe. In fact the fluid is handled as a solid travelling through the pipe at constant velocity. Similar assumptions were made by other researchers [1]. If we use the finite element technics for the formulation of the weak from of the equations of motion derivated from the above assumptions with proper shape functions [2] we can write the displacement as follows

$$u^{(e)} = \mathbf{N}_u^T \mathbf{q} \ , \quad \Theta^{(e)} = \mathbf{N}_\Theta^T \mathbf{q} \ , \quad \alpha^{(e)} = \mathbf{N}_\alpha^T \mathbf{q}$$

as functions of time dependent nodal q values. The integral expressions for the element matrices are as follows

$$[\mathrm{M}] = \int_0^L [(\rho_p A_p + \rho_f A_f)\mathrm{N}_u^T \mathrm{N}_u + (\rho_f I_f + \rho_p I_p)\mathrm{N}_\Theta^T \mathrm{N}_\Theta] dx \ ,$$

$$[\mathrm{B}] = \int_0^L \rho_f A_f v_0 \left[\mathrm{N}_u^T \frac{d\mathrm{N}_u}{dx} - \frac{d\mathrm{N}_u^T}{dx} \mathrm{N}_u \right] dx \ ,$$

$$[\mathrm{K}] = \int_0^L \left[E I_p \frac{d\mathrm{N}_\Theta^T}{dx} \frac{d\mathrm{N}_\Theta}{dx} + kGA_p \mathrm{N}_\alpha^T \mathrm{N}_\alpha - \rho_f A_f v_0^2 \frac{d\mathrm{N}_u^T}{dx} \frac{d\mathrm{N}_u}{dx} \right] dx \ .$$

Taking the variation of S equal to zero we shall have the expression

$$\delta S = \delta \mathrm{q}^T \int_0^t \left([\mathrm{M}] \frac{d^2\mathrm{q}}{dt^2} + [\mathrm{B}] \frac{d\mathrm{q}}{dt} + [\mathrm{K}]\mathrm{q} \right) dt = 0 \ .$$

As δq can be arbitrary we get the matrix equation

$$[\mathrm{M}] \frac{d^2\mathrm{q}}{dt^2} + [\mathrm{B}] \frac{d\mathrm{q}}{dt} + [\mathrm{K}]\mathrm{q} = 0 \ .$$

In the absence of structural of material damping, the damping matrix contains only gyroscopic coupling terms produced by Coriolis effects. The stiffness matrix includes terms originating from the bending and shear energy, and the centripetal acceleration of the fluid. The mass matrix is composed of terms arising from the transverse and rotary inertia of both the fluid and pipe. The final matrix equation has the general form of a complex eigenvalue problem or complex differential equation, in this case there is an external excitation. The contribution of Coriolis damping is an antisymmetric matrix. Inclusion of the Coriolis terms in the damping matrix differentiates this work from that of previous researchers [3]. The solution of the above equations cannot be done with the standard Systus algorithms. We have to use the nonsymmetrical Gauss algorithm for solving this problem. As the presence of velocity dependent Coriolis damping makes our problem nonlinear we had to develop a subroutine for our user defined pipe element. This FORTRAN subroutine was linked with Systus shared element library and we have got a new element [4]. Without Coriolis coupling (zero fluid velocity) this element behaves exactly like a standard type Systus beam element. In case we define cross section area, area moment of inertia, density and mean velocity of the fluid in MATERIAL PROPERTIES

and use the DAMPING label in transient nonlinear, our element will take into account the [**B**] matrix programmed in the above mentioned subroutine and modify [**M**] and [**K**] matrices with v_0 dependent terms.

This new element was tested in several ways. In the following we present a simple test and an industrial example as well.

3. Test Example

For testing the reliability of our new element we have defined a simple but demonstrative example where we can theoretically compute the effect of the Coriolis coupling.

This example was a ring of pipe elements in $x - y$ plane. All the elements were connected by rigid massless beams with the center point of the ring. We have allowed the rotation of the ring around an axis perpendicular to its plane and fixed against displacement and other rotations in the center of the ring. We have applied a constant 1 Nmm z torque on the axis which accelerated the model with a constant angular acceleration. The data of the model are the following:

Ring diameter = 1000 mm,
$\rho_f = 10^{-6}$ kgmm^{-3},
$A_f = 12.57$ mm^2,
Internal pipe diameter = 4 mm,
External pipe diameter = 5 mm.

As we could compute the inertial and mass quantities related to the model it was easy to compute ω in the 10th time step of integration when assuming a rigid body like motion around the rotational axis. This value was $1.0488\ 10^{-3}$ s^{-1}. Regarding the construction of the model we could assume that the model is dynamically balanced so we had not any reaction on the axis due to unbalance of inertia and mass. Therefore, if we regard the reactions on the axis we shall get exactly the sum of Coriolis forces acting on pipe elements. We have defined the flow direction of the fluid different on both halves of the model by inverting element axis y. Therefore, the sum of the Coriolis force has to be a $-x$ direction vector. This vector can be computed by the following integral

$$F_x = -4\rho_f A_f R\omega v_0 \int_{-\frac{\pi}{2}}^{\frac{\pi}{2}} \cos\varphi \, d\varphi \, .$$

If we take a $v_0 = 1000$ mm/s value this force will be $F_x = 1.13$ mN. We have computed F_x for fluid velocity $0, 1, \ldots, 10$ m/s. The results are presented

in *Fig. 1* and *Fig. 2*. We have used a $\tau = 1$ ms time step in the transient nonlinear method. The computed errors were found minor than 2 % when comparing the results to theoretical values.

4. Industrial Example

The so-called B type Coriforce flow meter is a standard product of MMG Co. Ltd. We have selected one geometry configuration from the existing product scale in order to compare its behaviour to model results. The model was simplified comparing to the real structure because we have neglected the flexibility of parts where Coriolis forces were not foreseen. The geometry is presented in *Fig. 3*. At the nodes marked by 13, 14, 15 and 16 we have modelled sensors like lumped masses. The model was fixed in four points. The flow direction is equal in the lower and upper parts. All the elements are of the new type. In the reality for the measurement – by exciting forces – the structure is maintained in a mode shape which is characterized by *Fig. 4* and is called butterfly mode. Practically, during the measurement it is enough to compare the z direction displacement functions of node pairs 13–15 or 14–16. The time shift between the zero crossings of these functions is a linear function of the fluid flow. The tube external and internal diameters were 31.75 and 29.67 mm, respectively. The material of the pipe and the eigenfrequency of the butterfly mode were steel and 96.02 Hz. In order to simulate the measuring situation without introducing the real controlling system into Systus we had to produce an initial state where the model shape and reactions were equal to the normalized butterfly mode. These initial conditions were computed by an equivalent model constructed from standard type pipe elements. From these initial conditions with transient nonlinear method we have computed time shift of first zero crossings between the above mentioned node pairs z directional displacement functions. The selected fluid velocity values were $0, 1, 2, \ldots, 10$ m/s. We have used several integration time steps. The values computed with 5^*10^{-5} s are to compared to measured ones in *Table 1*.

The errors of the computed values are the function of the selected time step. *Fig. 5* illustrates the effect of τ value selected. For $v_0 = 10$ m/s *Fig. 6* shows a 1/4 period of computed displacements at 13, 14, 15 and 16 nodes. *Fig. 7* is the appropriate zoom of *Fig. 6* for time shift measurement. Though the butterfly mode frequency of our model was exactly equal to the measured one we did not own measured values concerning the mode shape. Therefore we regard the computed errors very small. We made several geometrical simplifications in the model which might effect mainly

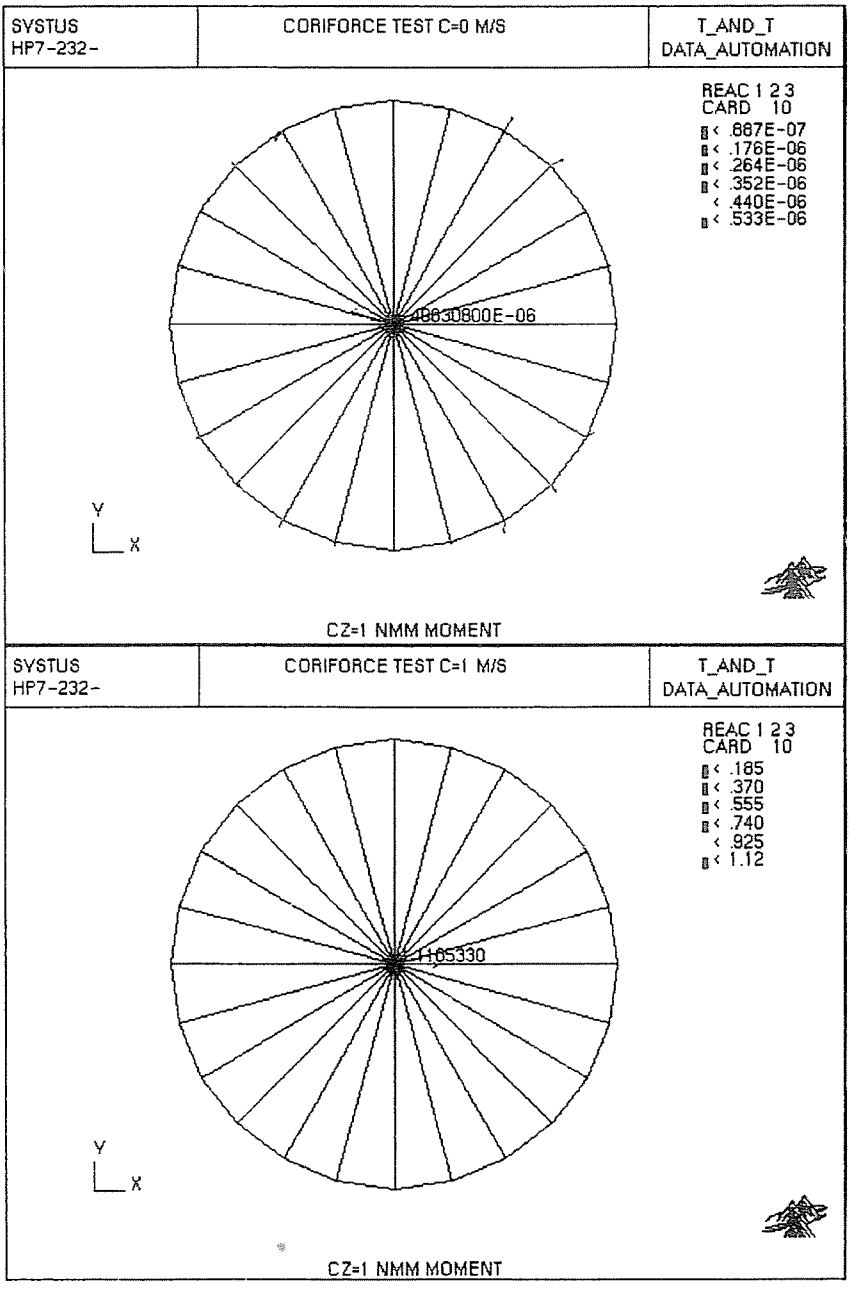

Fig. 1. Reaction forces for 0 and 1 m/s fluid velocities

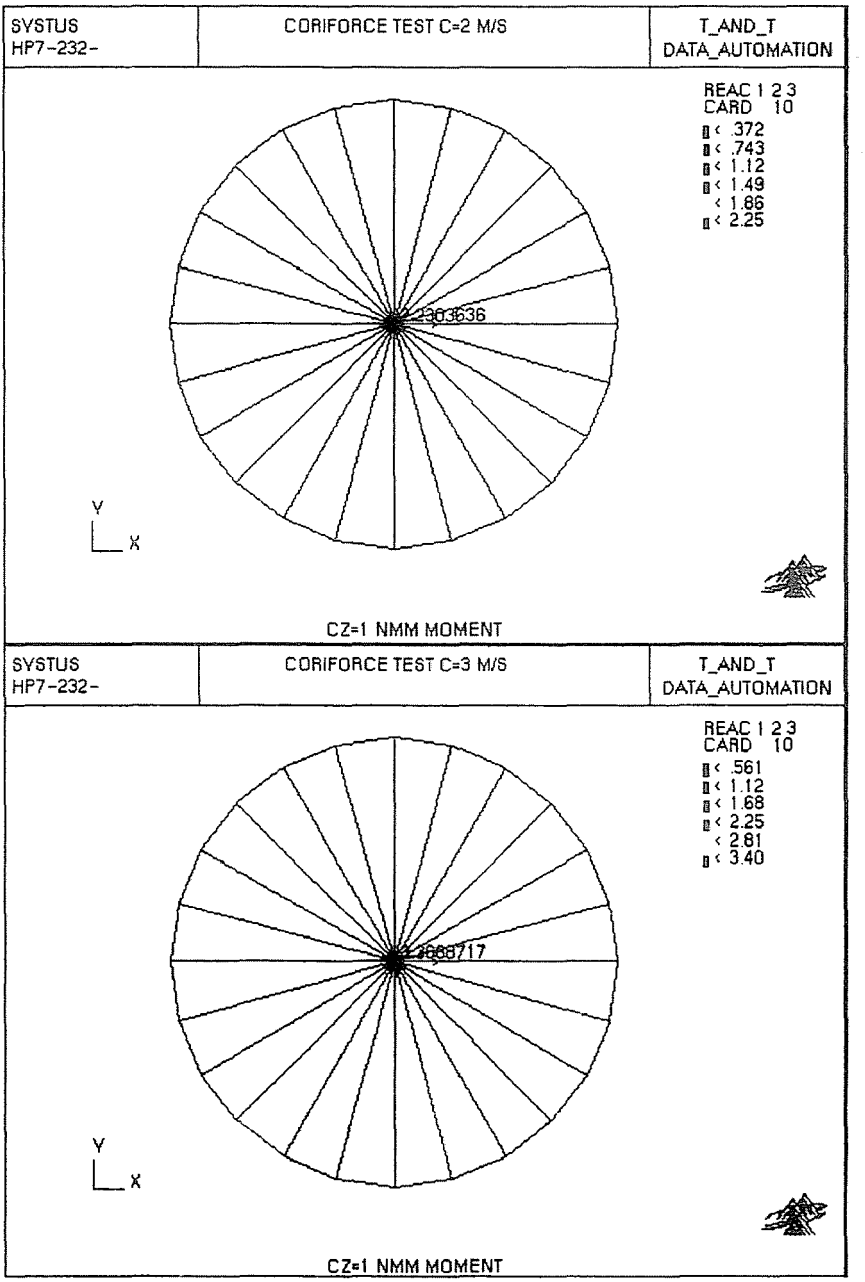

Fig. 2. Reaction forces for 2 and 3 m/s fluid velocities

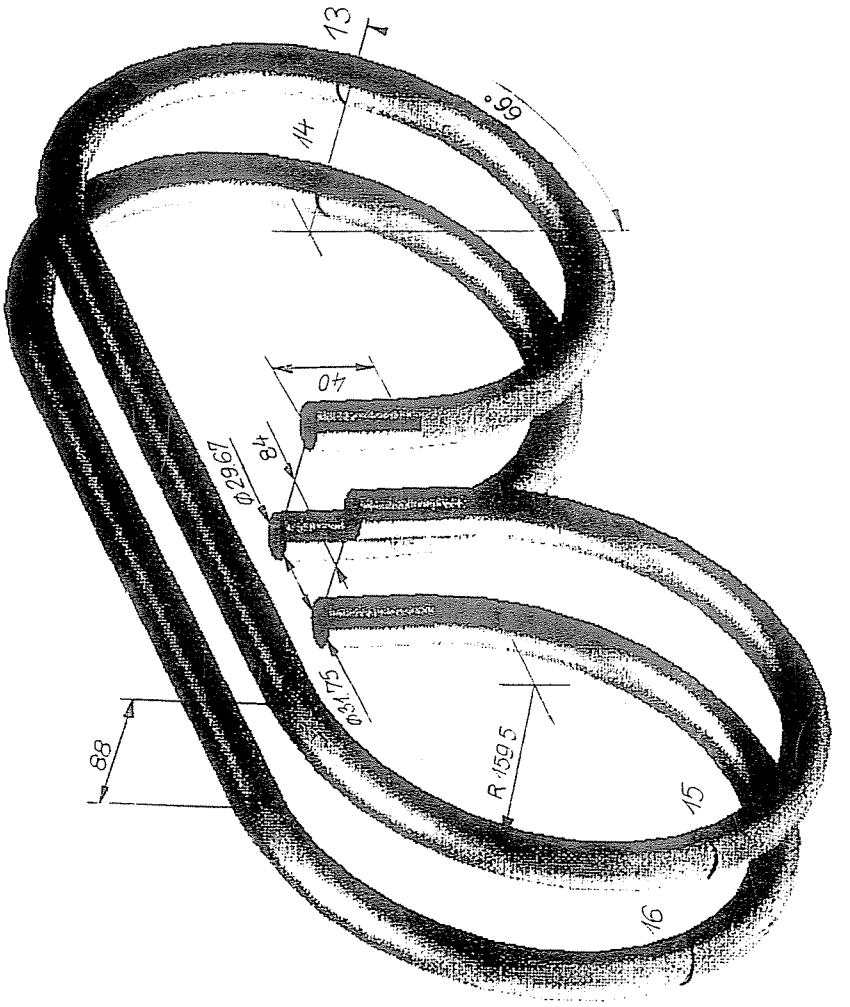

Fig. 3. Geometry of B form Coriforce flow meter

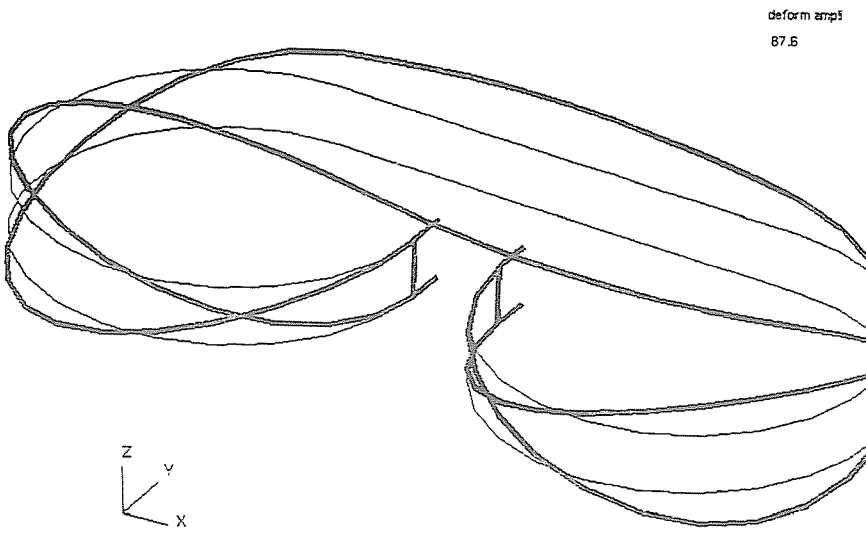

Fig. 4. Butterfly mode of 96.02 Hz eigenfrequency

Table 1
Measured and computed time shifts

Velocity of fluid [m/s]	Time shift*10^{-6} measured seconds	Time shift*10^{-6} computed seconds
1	6.73	6.75
2	13.5	13.1
3	20.2	18.9
4	26.9	25.9
5	33.6	32.4
6	40.4	39.5
7	47.1	45.4
8	53.8	51.9
9	60.5	59.5
10	67.3	66.5

the error magnitude. Probably with the use of a butterfly mode shape tuned with measured one we could achieve even higher accuracy.

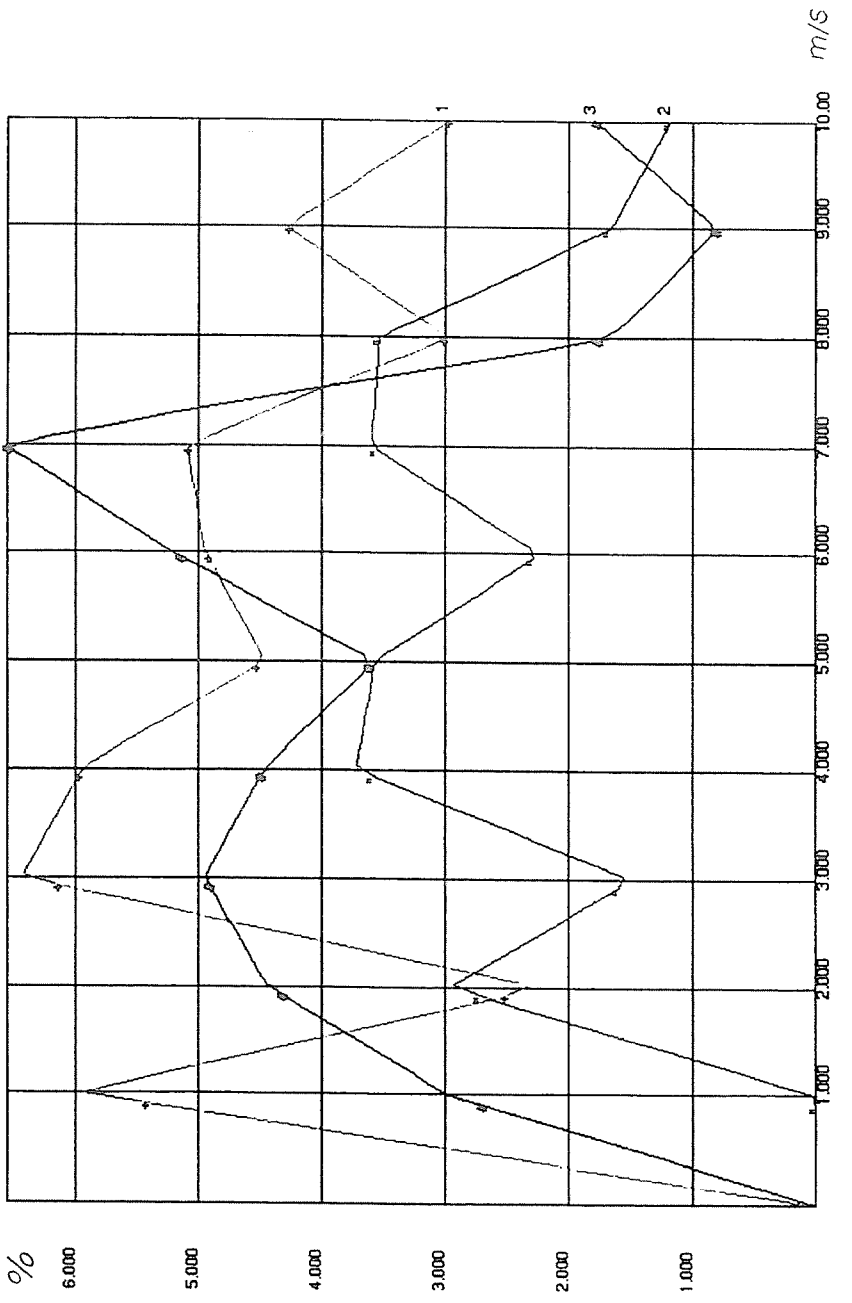

Fig. 5. Effect of integration time steps 0.1 ms, 0.05 ms and 0.025 ms. Difference in % between computed and measured time shifts

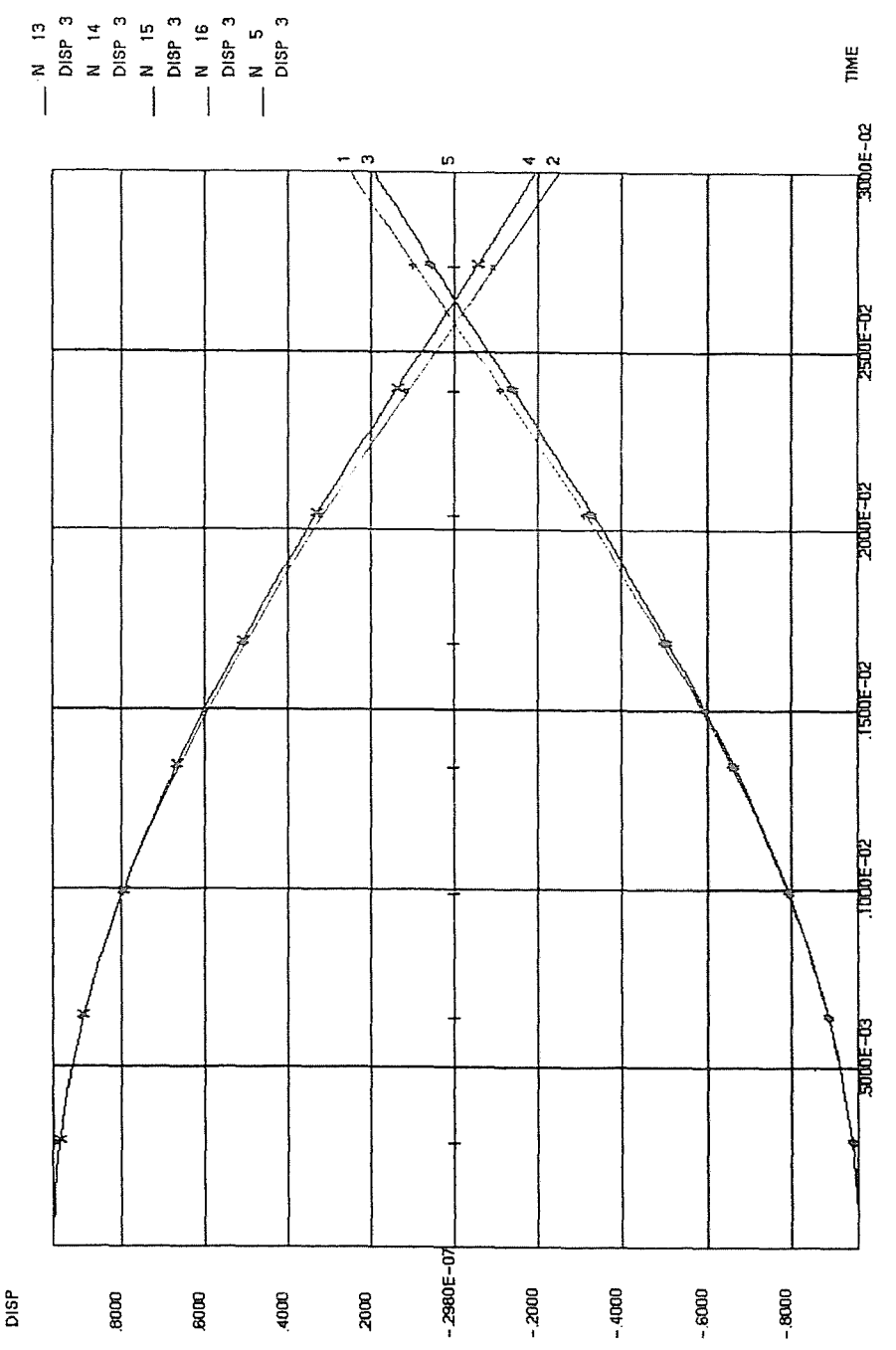

Fig. 6. Functions of z displacement computed at sensors in 13, 14, 15 and 16 nodes

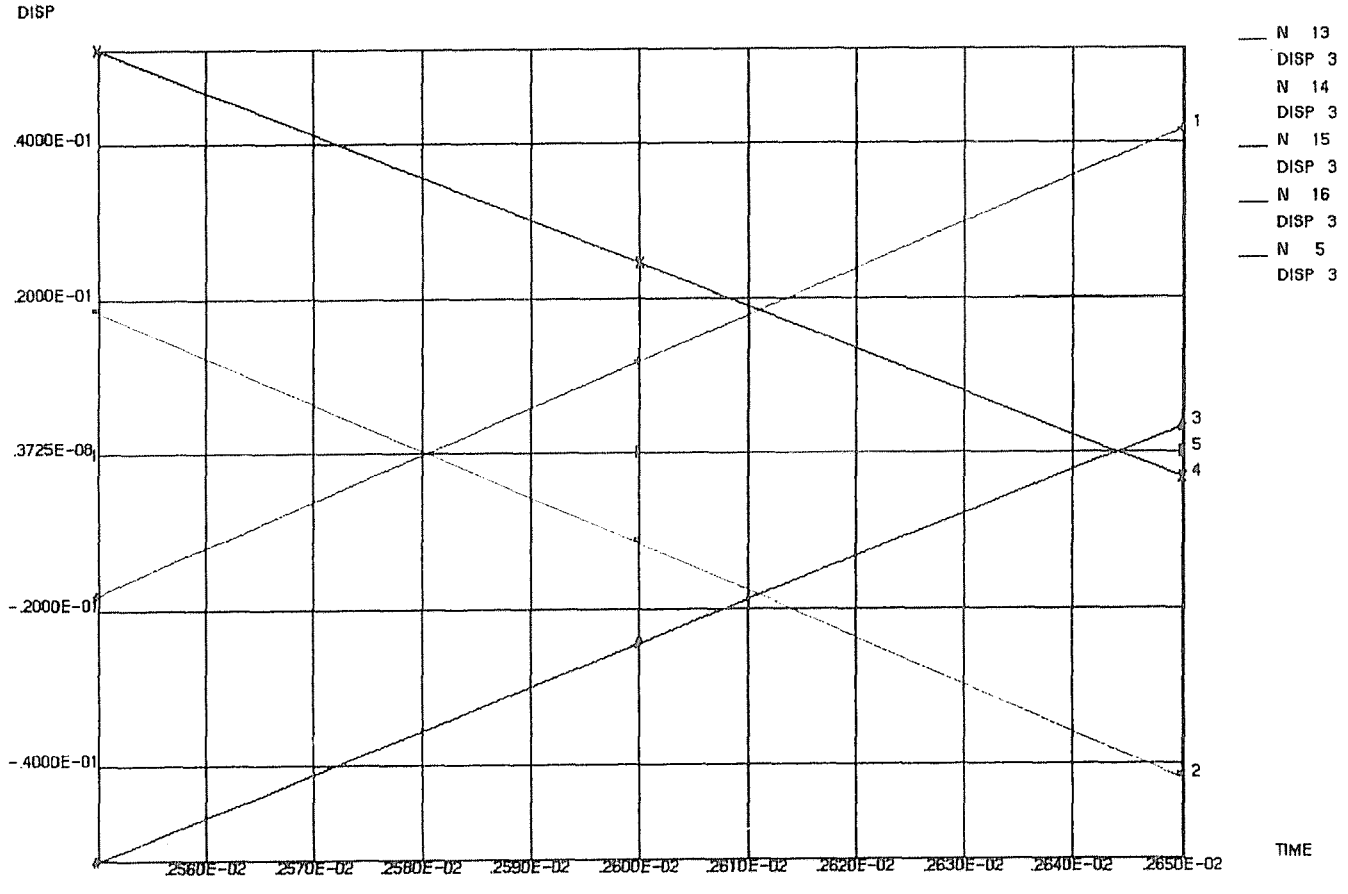

Fig. 7. Zoom of *Fig. 6* for visualizing time shift

5. Conclusions

Flow meter design is a difficult process. We do not have the knowledge how structural modifications of the flow meter will effect the resolution and sensitivity characteristics and how they influence the accuracy of our measurements. In order to reduce the number of expensive prototypes a reliable computer model has to be used. Generally structural optimization is made by finite element softwares. Unfortunately even the world leader softwares cannot handle Coriolis forces. The fact that SYSTUS has a shared element library has made possible that the authors could develop a new type element for MMG Co. Ltd whose behaviour was proved by measurements and theoretical test. There is a reason for standardize this new element in Systus because the presence of Coriolis forces is important for other fluid-conveying problems as well.

References

1. HUANG, C. C. (1974): Vibrations of Pipes Containing Flowing Fluids According to Timoshenko Theory. *Journal of Applied Mechanics*, September, pp. 814–817.
2. WEAVER, W. Jr. – JOHNSON, P. R. (1987): Structural Dynamics by Finite Elements. Prentice-Hall, 1987.
3. KOHLI, A. K. – NAKRA, B. C. (1984): Vibration Analysis of Straight and Curve Tubes Conveying Fluid by Means of a Straight Beam Finite Element. *Journal of Sound and Vibration*, Vol. 93, No. 2, pp. 307–311.
4. Systus User Manual (1993): Transient Nonlinear. Framsoft+CSI (Group Framatome), August.

Appendix

Shape Functions and Elemental Matrix Formulations

We assume the transversal displacement of our beam element has a cubic distribution over the element length,

$$u(x) = a_0 + a_1 x + a_2 x^2 + a_3 x^3 \ .$$

For the expression for the rotation due to flexural deformation over the element length we had the following distribution which assures constant shear strain,

$$\Theta(x) = a_1 + 2a_2 x + a_3(3x^2 + 6g) \ .$$

Here g is a constant determined from the material and geometry of the pipe

$$g = \frac{EI_p}{kGA_p}.$$

The coefficients a_0 to a_3 can be determined from transversal displacement and rotation at the ends $x = 0$ and $x = L$.

The lower triangles of elemental mass, stiffness and damping matrices are the following:

$$m_{11} = \frac{(\rho_p A_p + \rho_f A_f) L (1680 g^2 + 294 g L^2 + 13 L^4)}{35 (12 g + L^2)^2} + \\ + \frac{(\rho_p I_p + \rho_f I_f) 6 L^3}{5 (12 g + L^2)},$$

$$m_{21} = - \frac{(\rho_p A_p + \rho_f A_f) L^2 (1260 g^2 + 231 g L^2 + 11 L^4)}{210 (12 g + L^2)^2} - \\ - \frac{(\rho_p I_p + \rho_f I_f) L^2 (60 g - L^2)}{10 (12 g + L^2)^2},$$

$$m_{22} = \frac{(\rho_p A_p + \rho_f A_f) L^3 (126 g^2 + 21 g L^2 + L^4)}{105 (12 g + L^2)^2} + \\ + \frac{(\rho_p I_p + \rho_f I_f) 2 L (360 g^2 + 15 g L^2 + L^4)}{15 (12 g + L^2)^2},$$

$$m_{31} = \frac{(\rho_p A_p + \rho_f A_f) 3 L (560 g^2 + 84 g L^2 + 3 L^4)}{70 (12 g + L^2)^2} - \\ - \frac{(\rho_p I_p + \rho_f I_f) 6 L^3}{5 (12 g + g L^2)^2},$$

$$m_{32} = - \frac{(\rho_p A_p + \rho_f A_f) L^2 (2520 g^2 + 378 g L^2 + 13 L^4)}{420 (12 g + L^2)^2} - \\ - \frac{(\rho_p I_p + \rho_f I_f) L^2 (60 g - L^2)}{10 (12 g + L^2)^2},$$

$$m_{42} = - \frac{(\rho_p A_p + \rho_f A_f) L^3 (158 g^2 + 28 g L^2 + L^4)}{140 (12 g + L^2)^2} + \\ + \frac{(\rho_p I_p + \rho_f I_f) L (120 g^2 - 60 g L^2 - L^4)}{30 (12 g + L^2)^2},$$

$$m_{33} = m_{11}, \quad m_{41} = m_{32},$$

$$k_{11} = \frac{12 E I_p}{L^3 + 12 L g} - \frac{6 \rho_f A_f v_0^2}{5 L (L^2 + 12 g)^2} (120 g^2 + 20 g L^2 + L^4),$$

$$k_{21} = \frac{6EI_p}{L^2 + 12g} - \frac{\rho_f A_f v_0^2 L^4}{10(L^2 + 12g)^2} ,$$

$$k_{22} = \frac{4EI_p(L^2 + 3g)}{L^3 + 12Lg} - \frac{2L\rho_f A_f v_0^2}{15(L^2 + 12g)^2}(90g^2 + 15gL^2 + L^4) ,$$

$$k_{31} = -k_{11} ,$$
$$k_{32} = -k_{21} ,$$
$$k_{33} = k_{11} .$$
$$k_{41} = k_{21} ,$$

$$k_{42} = \frac{2EI_p(L^2 - 6g)}{L^3 + 12Lg} + \frac{L\rho_f A_f v_0^2}{30(L^2 + 12g)^2}(360g^2 + 60gL^2 + L^4) ,$$

$$k_{43} = -k_{21} .$$
$$k_{44} = k_{22} ,$$

$$b_{21} = \frac{\rho_f A_f v_0 L(10g + L^2)}{5(12g + L^2)} ,$$

$$b_{31} = -\rho_f A_f v_0 ,$$
$$b_{32} = b_{21} ,$$
$$b_{41} = -b_{21} ,$$

$$b_{42} = \frac{\rho_f A_f v_0 L^4}{360g + 30L^2} ,$$
$$b_{43} = b_{21} .$$